Available online at www.sciencedirect.com
ScienceDirect
Polymer 48 (2007) 1989–1997
polymer
www.elsevier.com/locate/polymer

Synthesis, characterization and application of well-defined environmentally responsive polymer brushes on the surface of colloid particles

Mingming Zhang [a], Li Liu [a,*], Chenglin Wu [a], Guoqi Fu [a], Hanying Zhao [b], Binglin He [a]

[a] *Key Laboratory of Functional Polymer Materials, Ministry of Education, Institute of Polymer Chemistry, College of Chemistry, Nankai University, Tianjin 300071, PR China*
[b] *Department of Chemistry, College of Chemistry, Nankai University, Tianjin 300071, PR China*

Received 10 November 2006; received in revised form 29 January 2007; accepted 31 January 2007
Available online 8 February 2007

Abstract

Well-defined poly(2-(dimethylamino) ethyl methacrylate) (PDMAEMA) brushes with high density were synthesized on the surface of polystyrene latex by atom transfer radical polymerization (ATRP) using acetone/water as the solvent and CuCl/$CuCl_2$/bpy as the catalyst. It was found that the polydispersity of PDMAEMA brushes decreased with the increasing external $CuCl_2$ concentration. The polymer brushes showed their lower critical solution temperature (LCST) at 31 and 33 °C under pH values of 10.0 and 8.0, respectively. Dynamic light scattering studies demonstrate that PDMAEMA brushes were pH- and salt-responsive. PDMAEMA domains were used as the nanoreactors to generate gold nanoparticles on the surface of colloid particles. TEM results indicate that monodispersed gold nanoparticles were obtained. These gold composite nanoparticles displayed effective catalytic activity in the reduction of 4-nitrophenol by $NaBH_4$.

Keywords: Polymer brushes; Atom transfer radical polymerization (ATRP); Gold nanoparticles

1. Introduction

Polymer brushes have recently attracted considerable attention due to their interesting properties and many potential applications. Controlled polymerization techniques such as ATRP allow the synthesis of various brushes with well-defined structures, controlled molecular weights and narrow polydispersities on planar and colloidal substrates [1–11]. Especially the stimuli-responsive polymer brushes synthesized by ATRP were of great interest for many applications in biotechnology and biomedical fields, because their properties can change with the environmental stimulus such as pH, temperature and salt concentration [12–18].

Poly(2-(dimethylamino) ethyl methacrylate) (PDMAEMA) is a pH- and temperature-sensitive polymer with a lower critical solution temperature (LCST) at around body temperature. Many researches have focused on the surface-initiated ATRP of DMAEMA and their potential applications [19–27]. Zheng et al. reported ATRP of DMAEMA from polymer microspheres and proposed that these particles have crucial importance in the binding and separation of proteins and other biomolecules [19,20]. In Chen's study, ATRP of DMAEMA from silica particles was carried out and the grafted particles were characterized by DLS, TGA, XPS and SEM, etc. These particles were stable at low or neutral pH, but aggregated at high pH values [21]. Xu et al. introduced a one-step process to prepare well-defined PDMAEMA brushes on the halogen-terminated single-crystal silicon surface. The modified single-crystal silicon has potential applications in the microelectronics industry [22]. Recently, ATRP of DMAEMA on

* Corresponding author. Tel.: +86 22 23501443.
E-mail address: nkliul@yahoo.com (L. Liu).

0032-3861/$ - see front matter © 2007 Elsevier Ltd. All rights reserved.
doi:10.1016/j.polymer.2007.01.069

various substrates such as Ge chips [23], poly(vinylidene fluoride) membrane [24], and carbon black [25] have also been described.

As one of the interesting applications, charged polymer brushes can be used to generate metallic nanoparticles within the brush layer using the confinement of gold or silver ion clusters. Ballauff and coworkers introduced Au, Ag and Pt nanoparticles attached to the spherical polyelectrolyte brushes. The properties and applications as catalysts were investigated in detail [28–30]. These immobilized metal nanoparticles are more stable and valuable in technological applications such as catalysis [29–32], sensors [33], drug delivery and protein adsorption [34].

In this paper, well-defined PDMAEMA brushes were generated from functionalized polystyrene latex by ''grafting-from'' technique. Scheme 1 shows the synthetic procedure. Firstly, seed polystyrene latex particles were prepared by emulsion polymerization. The ATRP initiator layer was prepared by seed emulsion polymerization of 2-(2-bromoisobutyryloxy) ethyl methacrylate (BIEM) using polystyrene (PS) latex as seeds. Next, the grafting of PDMAEMA chains was achieved by surface-initiated ATRP in acetone/H_2O at 35 °C. The average distance between neighboring PDMAEMA chains is much smaller than twice of the gyration radius (R_g) of a free polymer chain in solution, which means that the grafting density is in the brush regime. The aqueous solution behaviors of the PDMAEMA brushes were studied in detail. Additionally, the PDMAEMA brushes were used as nanoreactors to immobilize $AuCl_4^-$ ions. The reduction of these ions within the brush layer leads to the generation of monodispersed gold nanoparticles with an average size of approximately 4 nm on the surface of colloid particles. The catalytic activity of the gold composite nanoparticles was evaluated based on the reduction of 4-nitrophenol by an excess of $NaBH_4$.

2. Experimental

2.1. Materials

Styrene (Tianjin, P. R. China, AR) was washed with 5% NaOH aqueous solution, dried over anhydrous $MgSO_4$ and then vacuum-distilled from CaH_2. Divinylbenzene (DVB, Tianjin, P. R. China, 55%) was washed with 5% NaOH aqueous solution and dried over anhydrous $MgSO_4$. 2-(Dimethylamino) ethyl methacrylate (DMAEMA, Acros, 99%) was passed through a basic alumina column and dried with CaH_2. Hydroxylethyl methacrylate (HEMA) was purified through a basic alumina column and vacuum-distilled from Cu powder. CuCl (Tianjin, P. R. China, AR) was dissolved in concentrated HCl, precipitated by dilution with water, washed with ethanol and ethyl ether for three times, and then dried under vacuum. $CuCl_2$ (Tianjin, P. R. China, AR) was baked at 120 °C to remove the crystal water. Bipyridine (bpy) (Sinopharm Chemical Reagent Co., Ltd), ethyl 2-bromoisobutyrate (EBriB) (Aldrich, 98%), 2-bromoisobutyl bromide (Aldrich, 98%), $HAuCl_4 \cdot 4H_2O$ (Tianjin, P. R. China, AR) and $NaBH_4$ (Shanghai, P. R. China, 96%) were used without further purification. Potassium persulfate (KPS) was recrystallized in water. 4-Nitrophenol (Tianjin, P. R. China) was recrystallized from ethanol. All solvents were redistilled before use. Other reagents were used directly. 2-(2-Bromoisobutyryloxy) ethyl methacrylate (BIEM) was synthesized by the reaction of HEMA with 2-bromoisobutyryl bromide according to the literature [35].

2.2. Synthesis of ATRP initiator particles PS–PBIEM

Polystyrene (PS) latex particles were prepared by emulsion polymerization. Briefly, styrene (5 mL, 4.5 g), DVB (0.25 mL,

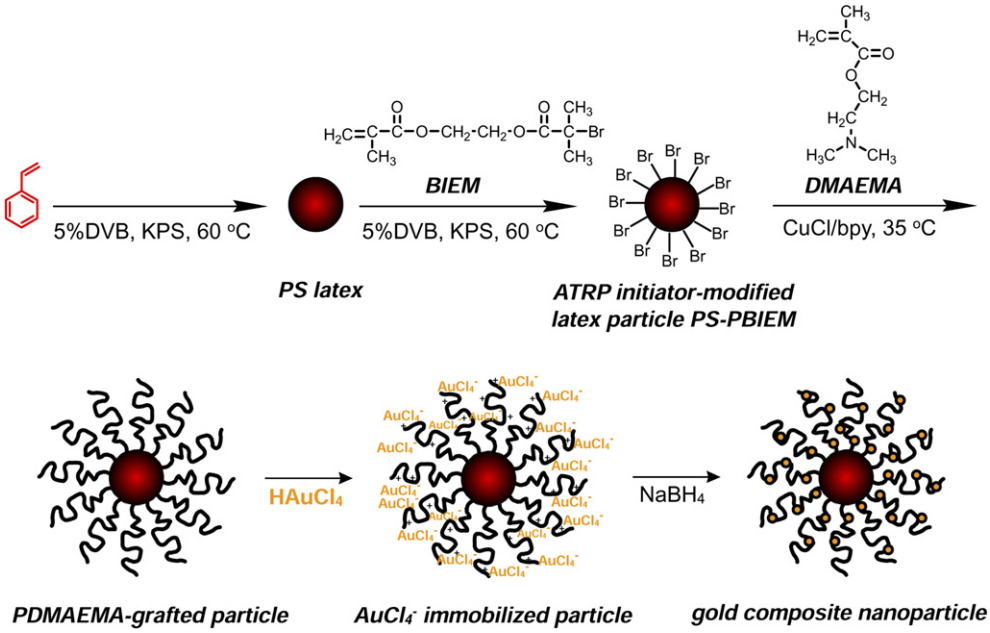

Scheme 1. Synthesis of PDMAEMA brushes on the surface of colloid particles by ATRP.

0.225 g), H_2O (100 mL), and sodium dodecyl sulfate (SDS) (0.6 g) were mixed together and purged with nitrogen for 30 min. After KPS (0.05 g) was added, the solution was stirred for 2 h at 60 °C. ATRP initiator particles PS–PBIEM were prepared by seeded emulsion polymerization of BIEM using polystyrene latex as seeds [36]. Briefly, BIEM (1 g) and DVB (0.05 g) were added to a suspension of PS latex particles (13.7 mL, containing 0.5 g PS). The mixture was purged with nitrogen for 30 min, followed by adding KPS (0.01 g). The reaction proceeded at 60 °C under nitrogen for 7 h. The resulting particles were precipitated in methanol, centrifuged at 10,000 rpm and washed with warm water. Before polymerization, the particles were redispersed in the solvent.

2.3. ATRP of DMAEMA from PS–PBIEM initiator latex particles

A typical procedure for the synthesis of PDMAEMA-grafted particles is described as follows. Acetone/water (92/8, v/v) suspension of initiator particles (2.17 mL, 3.2 wt%), 0.17 mL acetone solution of EBriB (3.4 μmol) used as a sacrificial initiator, and 2.33 mL (2.17 g, 13.8 mmol) DMAEMA were added in a 10 mL flask and the mixture was degassed by three freeze-pump-thaw cycles. CuCl (0.0195 g, 0.1967 mmol) and 0.0614 g (0.3934 mmol) bpy were added and the flask was degassed by another two freeze-pump-thaw cycles. Afterwards, the dark red mixture was stirred at 35 °C under nitrogen for 11 h. The viscous suspension was diluted with methanol, centrifuged at 14,000 rpm and washed with methanol until the precipitated particles became almost white. The resulting particles were dried under vacuum overnight. The combined supernatant was purified through a silica gel column and the solvent was evaporated to obtain the free PDMAEMA. The total conversion of DMAEMA was calculated from the following equation:

$$\text{Conversion}\ (\%) = \frac{W_{\text{total PDMAEMA}}}{W_{\text{DMAEMA}}} \times 100\% = \frac{W_{\text{grafted}} + W_{\text{free}}}{W_{\text{DMAEMA}}} \times 100\% \quad (1)$$

where W_{grafted} is the weight of grafted PDMAEMA calculated by the weight difference between the grafted particles and the initiator particles.

2.4. Synthesis of gold nanoparticles on the surface of PDMAEMA-grafted particles

An aqueous solution of $HAuCl_4 \cdot 4H_2O$ (1 mM) was added to a 1 mL aqueous solution of PDMAEMA-grafted particles (3.7 mg/mL) at different Au/N molar ratios (1:10 and 1:20). After stirring for 25 min, an aqueous solution of sodium borohydride ($NaBH_4$) (10 mM) ($NaBH_4/HAuCl_4$, molar ratio = 2.0) was added to the mixture and the solution immediately turned red-brown indicating the formation of gold nanoparticles. The solution was stirred for 1 h for completion of the reduction. The resulting gold nanoparticles were dialyzed against deionized water for 3 days (MWCO 12,000–14,000) to remove extra $NaBH_4$.

2.5. Catalytic reduction of 4-nitrophenol

One milliliter of freshly prepared aqueous solution of $NaBH_4$ (40 mM) was introduced in 2 mL aqueous solution of 4-nitrophenol (0.1 mM). Then, 0.255 mL of the gold composite nanoparticles (1.1 mg/mL) was added to the above solution under stirring. The absorption spectra were recorded by a Shimadzu UV-2104PC UV–vis scanning spectrophotometer at certain time interval in a scanning range of 250–500 nm at room temperature. The blank aqueous solution of gold composite nanoparticles was used as the reference.

2.6. Characterizations

^{1}H NMR measurement was performed on a Varian UNITY-plus 400M NMR spectrometer using $CDCl_3$ as the solvent. The molecular weight and polydispersity of free PDMAEMA were determined by gel permeation chromatography (GPC) with a Waters 510 pump and a Waters 410 refractive index detector. Dimethyl formamide (DMF) was used as the mobile phase at a flow rate of 1 mL/min. Polymer solution (200 μL) was injected through PL Mixed-B column at 45 °C. The data were processed by Waters Millennium station. Dynamic light scattering (DLS) measurements were performed on a laser light scattering spectrometer (BI-200SM) equipped with a digital correlator (BI-9000AT) at 532 nm. Transmission electron microscopy (TEM) images of gold composite nanoparticles were obtained on a Tecnai G^2 20 S-TWIN electron microscope equipped with a Model 794 CCD camera (512 × 512). All TEM images were obtained at an operating voltage of 200 kV. The determination of the lower critical solution temperature (LCST) was carried out on a Shimadzu UV-2101PC UV–vis spectrophotometer equipped with a Julabo F12 temperature control unit. The transmittance of aqueous solution of PDMAEMA-grafted particles was measured under different temperatures at a wavelength of 600 nm. The LCST values were determined as the onset temperature of the cloud point curves.

3. Results and discussion

3.1. Synthesis of PDMAEMA polymer brushes on PS colloid particles by ATRP

Cross-linked PS latex particles with ATRP initiator layer were obtained by seeded emulsion polymerization of 2-(2-bromoisobutyryloxy) ethyl methacrylate (BIEM) using PS latex as seeds [36]. The average diameter of the initiator particles was 50 nm determined from TEM images and the initiator content on the latex particles was calculated to be 2.46 mmol/g of particles based on the bromine content measured by elementary analysis (Chncorder-MF-3). Cross-linked polystyrene (PS) latex particles were chosen as the support for the growth of polymer brushes due to the large specific surface areas and

high stability in both aqueous and organic solvents. Additionally, polyelectrolyte-functionalized colloid particles are well suited for the immobilization of biomacromolecules and metal nanoparticles.

Using CuCl/bpy as the catalyst and acetone/water as the solvent, ATRP of DMAEMA was initiated from functionalized PS latex particles at 35 °C. ^{1}H NMR is employed to analyze the structure of the PDMAEMA-grafted particles (Fig. 1). The chemical shifts at δ 2.3 and 2.6 ppm are attributed to the methyl and methylene groups on the tertiary amine, respectively. The signal at δ 4.1 ppm corresponds to the methylene group adjacent to the carboxylate group of PDMAEMA. ^{1}H NMR analysis results confirm the successful polymerization of DMAEMA on the surface of colloid particles. To monitor the molecular weight of PDMAEMA grafted on the particles, free EBriB was added as a sacrificial initiator because it was reported that free polymers formed in solution have the same molecular weight as those formed on the surface assuming fast exchange between the two populations of polymers in the same system [5,8,25]. Table 1 summarizes the polymerization results under a variety of conditions. As shown in Table 1, the polydispersity index (PDI) of PDMAEMA was as high as 2.14 without external Cu^{2+}. However, the PDI decreased to 1.36 upon addition of 10 mol% Cu^{2+} (relative to the amount of CuCl). With further increasing the concentration of Cu^{2+} to 50 and 100 mol%, PDI reached 1.21 and 1.12, respectively. Therefore, the addition of external Cu^{2+} complex led to a better control of the polymerization process. Without external Cu^{2+}, the activation rate is much faster than the deactivation rate due to the low concentration of Cu^{2+} at the beginning of the reaction, which results in a high radical concentration and then termination. Adding Cu^{2+} and free initiator EBriB to the reaction media favors the deactivation rate and suppresses the radical termination at the early stage [37,38]. The polymerization can proceed smoothly with a constant radical concentration and well-defined polymers with low PDI can be obtained.

Grafting density of tethered polymer chains is an important parameter to determine the property of the polymer-grafted surface. The grafting density (σ) was calculated from the total mass of grafted polymer per unit area on the surface using the following equation:

$$\sigma\left(\text{chains}/\text{nm}^2\right) = \frac{10^{-21}\frac{W_1}{M_n}N_A}{\frac{W_0}{V_0\rho}4\pi R^2} \quad (2)$$

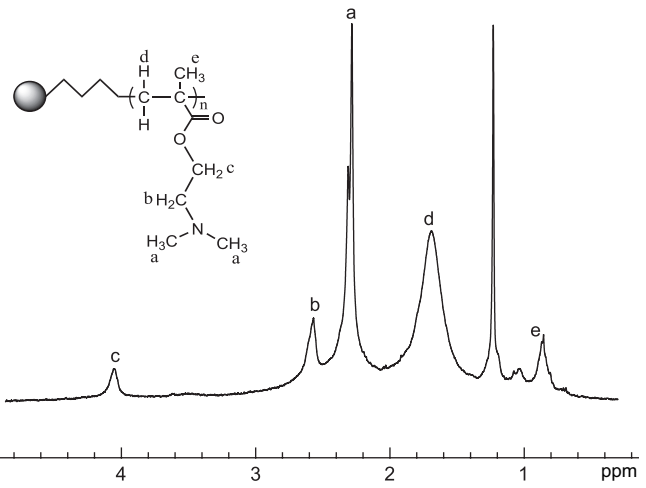

Fig. 1. ^{1}H NMR spectrum of PDMAEMA-grafted particles in $CDCl_3$.

Herein, W_1 is the weight of PDMAEMA grafted on the polystyrene latex particles and W_0 is the weight of initiator particles; V_0 (cm^3) is the volume of the initiator latex particles calculated by $V_0 = 4\pi r^3/3$, where r is the average radius of the initiator latex particles measured by TEM (25 nm); ρ is the particle density (1.1 g/cm^3) [4]; N_A is the Avogadro's number; R is the radius of the grafted particles, with the value of 25 nm at the surface of latex particles.

The average distance between neighbor chains (D) is described as $\sigma^{-1/2}$. As shown in Table 2, D/R_g values of all samples are much less than 2, which illustrates that the grafting density of PDMAEMA synthesized by surface-initiated ATRP from colloid particles is in the brush regime [5].

3.2. LCST of PDMAEMA brushes and dependence on pH

UV–vis spectroscopy was used to monitor the transmittance of PDMAEMA brushes in aqueous solution at different pHs and temperatures. The particle concentration was kept at 0.025 wt% in all tests. The temperature dependence of the transmittance for the PDMAEMA brushes at various pH values is shown in Fig. 2. At pH 3.0, the transmittance of the particle solution is almost unchanged with the increasing temperature. So, PDMAEMA brushes have no temperature-sensitive character at pH 3.0. But at pH 10.0, PDMAEMA brushes are thermal responsive and have a LCST at about 31 °C. As temperature was raised above 32 °C, the increasing

Table 1
ATRP of DMAEMA using CuCl/bpy as the catalyst and acetone/water (92/8, v/v) as the solvent

Entry	Cu^{2+}/Cu^{+} (mol%)	Sacrificial initiator (μmol)	Time (h)	Monomer conversion[a] (%)	Graft[b] (%)	M_n[c]	PDI (M_w/M_n)[c]
1	0	3.4	8.5	83	36	71,000	2.14
2	10	6.7	9.5	100	8.7	51,000	1.36
3	50	3.4	11	65	18	39,000	1.21
4	100	3.4	28	47	24	47,000	1.12

Other polymerization conditions: 0.07 g initiator particles (net weight), 0.20 mmol CuCl, bpy = 2(CuCl + $CuCl_2$), 35 °C.

[a] Total conversion of DMAEMA.

[b] The amount of PDMAEMA grafted on the particles = graft polymer/total polymer.

[c] M_n, M_w/M_n of the free PDMAEMA produced by EBriB in solution.

Table 2
Grafting density (σ), distance between the grafted chains (D) and D/R_g of tethered PDMAEMA chains on the surface of latex particles

Entry	Graft density σ (chains/nm^2)	D[a] (nm)	R_g[b] (nm)	D/R_g
1	0.88	1.07	11.3	0.09
2	0.33	1.73	9.0	0.19
3	0.83	1.10	7.9	0.14
4	0.49	1.44	11.8	0.12

[a] Distance between the grafted chains $D = \sigma^{-1/2}$.
[b] R_g: radius of gyration estimated by $R_g = 0.5N^{0.5}$ (N: polymerization degree, Ref. [39]).

of transmittance was caused by the aggregation and sedimentation of particles due to the absence of steric/electrostatic repulsive stabilizations of PDMAEMA brushes for the colloid particles. Because the PDMAEMA brushes are more hydrophilic at pH 8.0 than at pH 10.0, the LCST shifts to a higher temperature 33 °C. However, the transmittance decreases only slightly above LCST, indicating that PDMAEMA brushes are less thermo-sensitive at pH 8.0 than at pH 10.0.

3.3. Influences of pH and salt on PDMAEMA brushes in aqueous solutions

The hydrodynamic radii of both initiator particle (r_h) and PDMAEMA-grafted particle (R_h) were determined by dynamic light scattering (DLS). The hydrodynamic radius value was the average of three measurements. The r_h is 42.5 nm and maintains constant at different pHs. Thereby, the brush thickness (L) at certain pH is calculated by the difference between R_h and r_h. The pH dependence of the thickness of the PDMAEMA brushes is displayed in Fig. 3. It can be seen that the brush thickness decreases markedly with the increase of pH. At pH 3.0, the PDMAEMA chains are entirely protonated and highly stretch along the radial direction due to the geometrical constraint and the electrostatic repulsion between

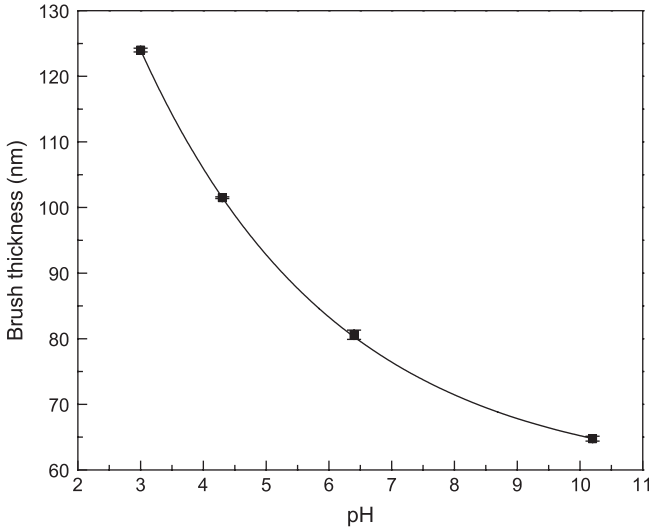

Fig. 3. pH dependence of the thickness of the PDMAEMA brushes at 25 °C. Entry 3 was used for the DLS measurement.

polymer chains. As pH changes from 3.0 to 10.5, PDMAEMA chains gradually shrink from solution due to the deprotonation of amine groups. As a result, the brush thickness decreases from 124 to 65 nm. The DLS studies demonstrate that PDMAEMA brushes are pH-sensitive.

Salts are known to influence the properties of polyelectrolyte aqueous solution, since they disrupt the hydration structure surrounding the polymer chains. Sodium chloride (NaCl) is a typical example of destroying the hydration sheath near the polymer chains. Therein, the influence of NaCl on the PDMAEMA brush thickness was investigated.

Fig. 4 shows the dependence of the PDMAEMA brush thickness on NaCl concentration. The brush thickness decreases with increasing NaCl concentration. In the absence of salt at pH 3.0, the PDMAEMA chain is totally ionized and stretches to nearly full length due to the high osmotic

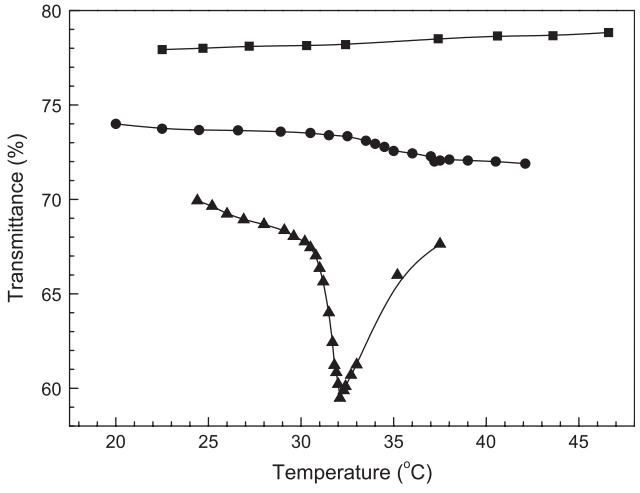

Fig. 2. Temperature dependence of the transmittance of the PDMAEMA-grafted particles at pH 3.0 (−■−), 8.0 (−●−) and 10.0 (−▲−) determined by UV−vis spectroscopy. Entry 3 was used for the UV−vis detection and the wavelength was setup at 600 nm.

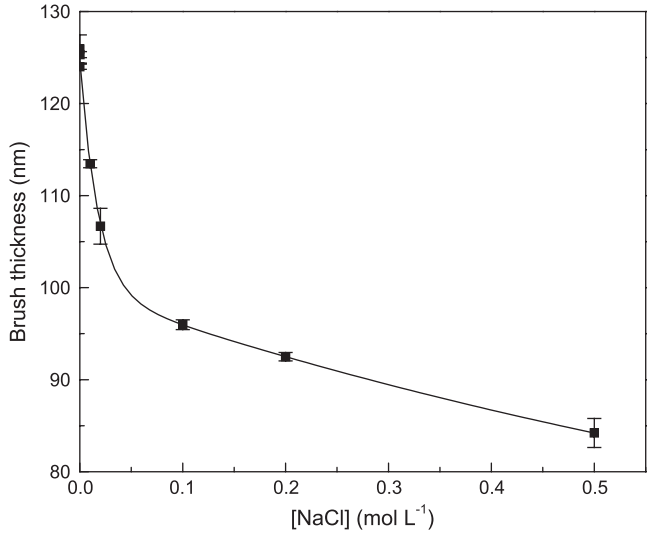

Fig. 4. [NaCl] dependence of the thickness of the PDMAEMA brushes at pH 3 under 25 °C. Entry 3 was used for the DLS measurement.

pressure and electrostatic repulsion. The addition of salt progressively screens the charge within the brush layer, which leads to the shrinking of the PDMAEMA chains. The brush thickness as a function of $[NaCl]^{-1/3}$ is shown in Fig. 5. Beyond 0.01 M NaCl, the brush is in the salted regime and a well linear relationship between the brush thicknesses and $[NaCl]^{-1/3}$ is found. This result is in good agreement with scaling theory in the salted brush regime [40,41].

3.4. Synthesis of gold nanoparticles on the surface of PDMAEMA-grafted particles

The synthesis of gold nanoparticles was carried out in aqueous solutions of PDMAEMA-grafted particles by reduction of hydrogen tetrachloroaureate(III) ($HAuCl_4 \cdot 4H_2O$) at room temperature. After adding $NaBH_4$, the solution immediately became light orange-red in color and the color didn't change with the reaction time, indicating that the reduction of the Au(III) to Au(0) was very fast. Alternatively, it is also known that PDMAEMA is able to facilitate autoreduction of the auric cations to obtain gold nanoparticles without any additional reducing reagent [42]. So gold nanoparticles incorporated in PDMAEMA brushes were also prepared without addition of $NaBH_4$. The particle solution showed light pink-red in about 0.5 h, and the reaction was kept for about 5 h while the color became purple-red. The previous method was a kind of fast reduction method, and the latter one was a slow reduction method.

The formation of gold nanoparticles was monitored by recording the changes in the absorption spectra centered at ~530 nm on a UV–vis spectrometer. Fig. 6 shows the UV–vis spectra of the gold nanoparticles prepared at Au/N molar ratio 1:20 with and without $NaBH_4$. The resonance plasmon of gold nanoparticles prepared with $NaBH_4$ appears only as a shoulder in the UV–vis spectrum at about 510 nm. In contrast, the one prepared without adding $NaBH_4$ shows an absorption band at ~530 nm. This implies that the size of gold nanoparticles prepared in the absence of $NaBH_4$ is much larger than that prepared with $NaBH_4$.

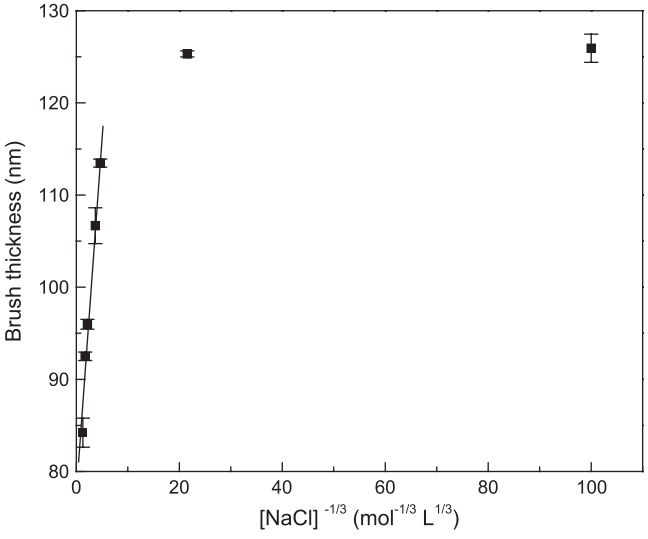

Fig. 5. $[NaCl]^{-1/3}$ dependence of the thickness of the PDMAEMA brushes at pH 3 under 25 °C. Entry 3 was used for the DLS measurement.

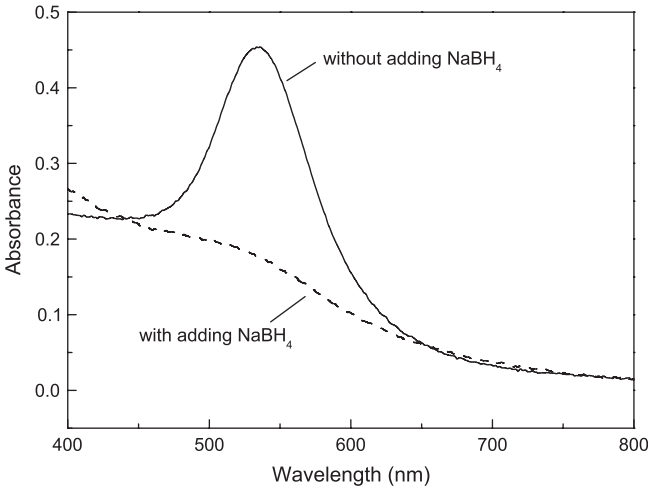

Fig. 6. UV–vis spectra of gold nanoparticles prepared on PDMAEMA-grafted particles at Au/N molar ratio 1:20 with and without $NaBH_4$.

From TEM images (Fig. 7), we can clearly see that the gold nanoparticles prepared in the presence of $NaBH_4$ are much smaller. The gold nanoparticles prepared without any reducing agents have an average diameter of 19.6 nm (Fig. 7A and B) and the size distribution is 1.62 (Fig. 7C). The gold nanoparticles obtained by $NaBH_4$ reduction method have an average diameter of 4.2 nm (Fig. 7D and E) and monodispersity (1.12) (Fig. 7F). The addition of $NaBH_4$ into the solution led to the formation of gold crystal seeds in short time, and the nucleation of the gold nanoparticles took place on many spots on the surface of particles, so smaller particles could be obtained in comparison with those grown without adding any reducing agents under the same conditions. Moreover, the narrow size distribution indicates that the nucleation and growth of gold nanoparticles proceeded practically instantaneously. TEM results from Fig. 7D and E demonstrate that all gold nanoparticles are located near the surface of the core particles, indicating that the nucleation and growth of gold nanoparticles occur within the brush layer. This means that the PDMAEMA brushes act as the nanoreactors for the production of gold nanoparticles. As seen from these TEM images, no aggregation of the nanoparticles takes place on the surface. The prepared gold composite nanoparticles are very stable at room temperature, and no precipitation is observed over several weeks, which confirms that the gold nanoparticles are immobilized within the polymer brushes. The densely packed PDMAEMA brushes and the interaction between gold nanoparticles and polymer chains are contributed to the stabilization of gold nanoparticles.

3.5. Catalytic reduction of 4-nitrophenol

As one of the interesting applications, the catalytic properties of these gold composite nanoparticles were investigated

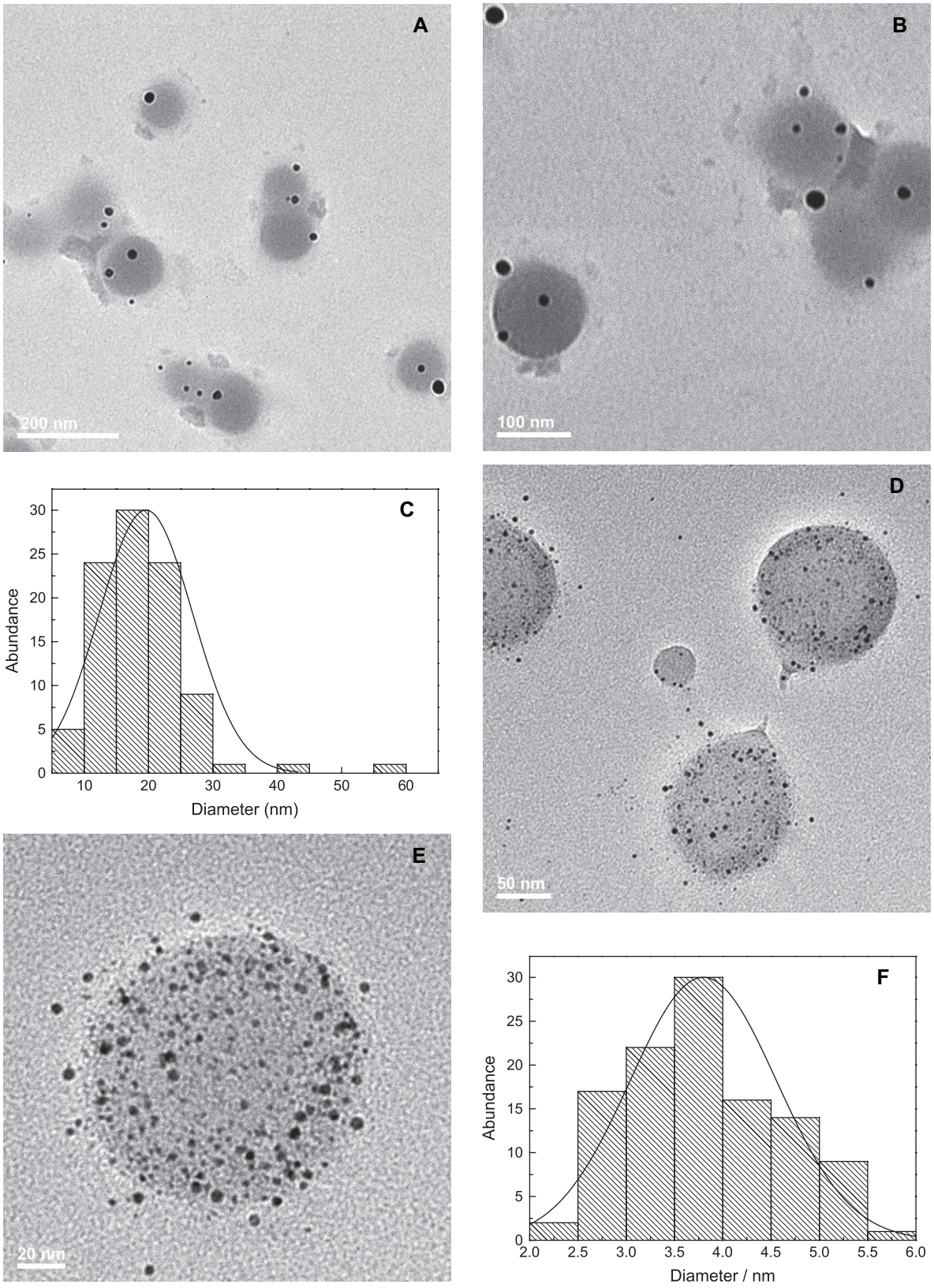

Fig. 7. TEM images of the gold composite nanoparticles prepared without (A, B) and with adding $NaBH_4$ (D, E) and their size distributions are shown in C and F, respectively.

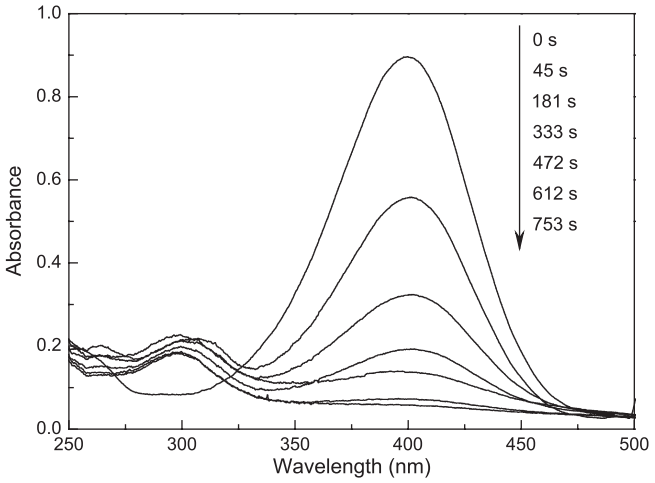

Fig. 8. UV–vis absorption spectra of the reduction of 4-nitrophenol catalyzed by gold composite nanoparticles. Conditions: [4-nitrophenol] = 0.06 mM, [$NaBH_4$] = 12 mM, Au-particles = 0.086 mg/mL.

based on the reduction of 4-nitrophenol by sodium borohydride because the resulting substance 4-aminophenol is a commercially important intermediate for the manufacture of analgesic and antipyretic drugs. After adding $NaBH_4$ into the aqueous solution of 4-nitrophenol, the solution color changed from light yellow to yellow-green due to the formation of 4-nitrophenolate ion. The yellow-green color remained unaltered in the absence of any catalysis. But after addition of the gold composite nanoparticles to the reaction media, the color of the 4-nitrophenolate ions faded with time. The process of reduction was monitored by UV–vis spectra. Fig. 8 displays the successive absorption UV–vis spectra of the reduction of 4-nitrophenol catalyzed by gold composite nanoparticles. The characteristic peak of the 4-nitrophenolate ions at 400 nm decreased with time, and a new peak gradually developed at 300 nm that corresponds to 4-aminophenol [32]. The reduction reaction was practically finished in 13 min.

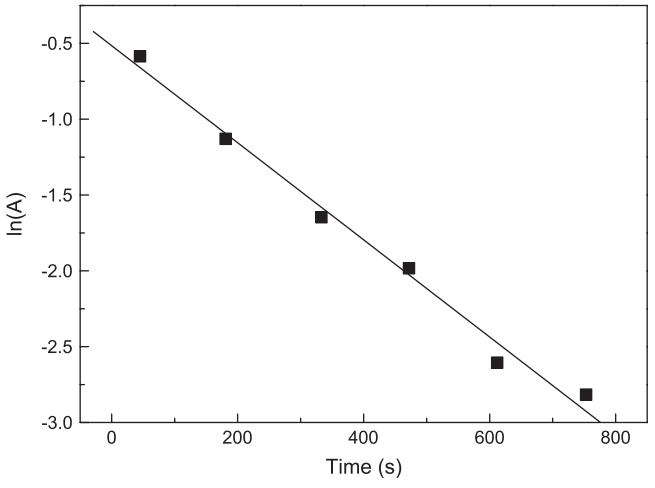

Fig. 9. Plot of ln(A) versus time for the reduction of 4-nitrophenol catalyzed by gold composite nanoparticles. Conditions: [4-nitrophenol] = 0.06 mM, [$NaBH_4$] = 12 mM, Au-particles = 0.086 mg/mL.

The catalysis mechanism is attributed to the efficient gold nanoparticle-mediated electron transfer from BH_4^- ion to nitro compounds [31].

Since the concentration of $NaBH_4$ is in excess compared to 4-nitrophenol, it can be assumed constant during the reaction. Therefore, pseudo-first-order kinetics with respect to 4-nitrophenol can be used to evaluate the catalytic rate. A good linear correlation between ln(A) (A is absorbance at any time) and reaction time was achieved (Fig. 9). The pseudo-first-order rate constant (k) estimated from the plot is $3.2 \times 10^{-3}\ s^{-1}$. Similar results were also reported by Liu [31] and Hayakawa [32].

4. Conclusions

Well-defined PDMAEMA brushes were successfully produced on the surface of colloid particles by surface-initiated ATRP using CuCl/$CuCl_2$/bpy as the catalyst in acetone/water (92/8, v/v) at ambient temperature. The PDI decreased remarkably with increasing Cu^{2+} concentration. PDMAEMA brushes were thermo-responsive at basic pH and showed a LCST at 31 and 33 °C under pH 10 and 8, respectively. The thickness of PDMAEMA brushes decreased with the increase of solution pH or salt concentration, demonstrating pH- and salt-sensitive characteristics. Due to the environmentally responsive properties of the polymer brushes, the PDMAEMA-grafted colloid particles have potential applications in biotechnology and bioseparations. Using PDMAEMA brushes as the nanoreactor, monodispersed gold nanoparticles were generated on the surface of colloid particles with an average diameter of 4.2 nm and size distribution of 1.12. The gold composite nanoparticles displayed effective catalytic activity in the reduction of 4-nitrophenol by $NaBH_4$. The pseudo-first-order rate constant k was estimated to be $3.2 \times 10^{-3}\ s^{-1}$.

Acknowledgements

This project is supported by Start-up fund of Nankai University, and Science and Technology Committee of Tianjin under contract No. 05YFJMJC06700.

References

[1] Mori H, Seng DC, Zhang M, Müller AHE. Langmuir 2002;18:3682–893.
[2] Ohno K, Morinaga T, Koh K, Tsujii Y, Fukuda T. Macromolecules 2005;38:2137–42.
[3] Li D, Sheng X, Zhao B. J Am Chem Soc 2005;127:6248–56.
[4] Guerrini MM, Charleux B, Vairon JP. Macromol Rapid Commun 2000;21:669–74.
[5] Jayachandran KN, Raymond NJ, Brooks DE. Macromolecules 2004;37:734–43.
[6] Jayachandran KN, Kumar KR, Goodman D, Brooks DE. Polymer 2004;45:7471–89.
[7] Wang X, Tu H, Braun PV, Bohn PW. Langmuir 2006;22:817–23.
[8] Feng W, Chen R, Brash JL, Zhu S. Macromol Rapid Commun 2005;26:1383–8.

[9] Yang Y, Wu D, Li C, Liu L, Cheng X, Zhao H. Polymer 2006;47:7374–81.
[10] Hu D, Cheng Z, Zhu J, Zhu X. Polymer 2005;46:7563–71.
[11] Zhao H, Farrell BP, Shipp DA. Polymer 2004;45:4473–81.
[12] Sun T, Wang G, Feng L, Liu B, Ma Y, Jiang L, et al. Angew Chem Int Ed 2004;43:357–60.
[13] Xu FJ, Cai QJ, Li YL, Kang ET, Neoh KG. Biomacromolecules 2005;6:1012–20.
[14] Lee H-I, Pietrasik J, Matyjaszewski K. Macromolecules 2006;39:3914–20.
[15] Kim DJ, Heo J-Y, Kim KS, Choi IS. Macromol Rapid Commun 2003;24:517–21.
[16] Xu FJ, Zhong SP, Zhong LYL, Tong YW, Kang ET, Neoh KG. Biomaterials 2006;27:1236–45.
[17] Kurosawa S, Aizawa H, Talib ZA, Atthoff B, Hilborn J. Biosens Bioelectron 2004;20:1165–76.
[18] Seino M, Yokomachi K, Hayakawa T, Kikuchi R, Kakimoto M, Horiuchi S. Polymer 2006;47:1946–52.
[19] Zheng G, Stöver HDH. Macromolecules 2002;35:7612–9.
[20] Zheng G, Stöver HDH. Macromolecules 2003;36:7439–45.
[21] Chen X, Randall DP, Perruchot C, Watts JF, Patten TE, Werne TV, et al. J Colloid Interf Sci 2003;257:56–64.
[22] Xu FJ, Cai QJ, Kang ET, Neoh KG. Langmuir 2005;21:3221–5.
[23] Xu FJ, Cai QJ, Kang ET, Neoh KG, Zhu CX. Organometallics 2005;24:1768–71.
[24] Zhai G, Shi ZL, Kang ET, Neoh KG. Macromol Biosci 2005;5:974–82.
[25] Liu T, Jia S, Kowalewski T, Matyjaszewski K. Macromolecules 2006; 39:548–56.
[26] Cheng Z, Zhu X, Shi ZL, Neoh KG, Kang ET. Ind Eng Chem Res 2005;44:7004–98.
[27] Xu P, Kirk EAV, Li S, Murdoch WJ, Ren J, Hussain MD, et al. Colloids Surf B Biointerf 2006;48:50–7.
[28] Sharma G, Ballauff M. Macromol Rapid Commun 2004;25:547–52.
[29] Lu Y, Mei Y, Drechsler M, Ballauff M. Angew Chem Int Ed 2006;45:813–6.
[30] Mei Y, Sharma G, Lu Y, Ballauff M. Langmuir 2005;21:12229–34.
[31] Liu J, Qin G, Raveendran P, Ikushima Y. Chem Eur J 2006;12: 2131–8.
[32] Hayakawa K, Yoshimura T, Esumi K. Langmuir 2003;19:5517–21.
[33] Frederix F, Friedt J-M, Choi K-H, Laureyn W, Campitelli A, Mondelaers D, et al. Anal Chem 2003;75:6894–900.
[34] Phadtare S, Kumar A, Vinod VP, Dash C, Palaskar DV, Rao M, et al. Chem Mater 2003;15:1944–9.
[35] Matyjaszewski K, Gaynor SG, Kulfan A, Podwika M. Macromolecules 1997;30:5192–4.
[36] Zhang M, Liu L, Zhao H, Yang Y, Fu G, He B. J Colloid Interf Sci 2006;301:85–91.
[37] Jin X, Shen Y, Zhu S. Macromol Mater Eng 2003;288:925–35.
[38] Kajiwara A, Matyjaszewski K, Kamachi M. Macromolecules 1998;31: 5695–701.
[39] Uchida E, Ikada Y. Macromolecules 1997;30:5464–9.
[40] Wesley RD, Cosgrove T, Thompson L, Armes SP, Billingham NC, Baines FL. Langmuir 2000;16:4467–9.
[41] Israels R, Leermakers FAM, Fleer GJ. Macromolecules 1994;27:3087–93.
[42] Ishii T, Otsuka H, Kataoka K, Nagasaki Y. Langmuir 2004;20:561–4.